IEEE Access
Multidisciplinary | Rapid Review | Open Access Journal

Received January 14, 2020, accepted January 27, 2020, date of publication February 3, 2020, date of current version February 10, 2020.

Digital Object Identifier 10.1109/ACCESS.2020.2971086

Dual-Receiver Wearable 6.78 MHz Resonant Inductive Wireless Power Transfer Glove Using Embroidered Textile Coils

MAHMOUD WAGIH, (Graduate Student Member, IEEE), ABIODUN KOMOLAFE, AND BAHAREH ZAGHARI

School of Electronics and Computer Science, University of Southampton, Southampton SO17 1BJ, U.K.

Corresponding author: Mahmoud Wagih (mahm1g15@ecs.soton.ac.uk)

This work was supported by the U.K. Engineering and Physical Sciences Research Council (EPSRC) under Grant EP/P010164/1.

ABSTRACT The design of dynamic wearable wireless power transfer systems (WPT) possesses multiple challenges that affect the WPT efficiency. The varying operation conditions, such as the coils' coupling, and operation in proximity or through the human body, can affect the impedance matching at the resonant frequency. This paper presents a high-efficiency wearable 6.78 MHz WPT system for smart cycling applications. Resonant inductive coupling using dual-receiver textile coils is proposed for separation-independent WPT, demonstrated in a smart cycling glove, for transferring energy from an on-bicycle generator to smart-textile sensors. The effects of over-coupling in a dynamic WPT system have been investigated analytically and experimentally. The embroidered coils efficiency is studied in space, on- and through-body. The measured results, in space, show around 90% agreement between the analytical and experimental results. To overcome frequency-splitting in the over-coupling region, an asymmetric dual-receiver architecture is proposed. Empirical tuning of the lumped capacitors is utilized to achieve resonance at 6.78 MHz between the fundamental frequency and the even mode split frequency. Two different coil sizes are utilized to achieve separation-independent efficiency in the tight coupling region on- and off-body, while maintaining a Specific Absorption Rate (SAR) under 0.103 W/kg. The presented system achieves a peak efficiency of 90% and 82% in free space and on-hand respectively, with a minimum efficiency of 50% under loose and tight coupling, demonstrating more than 40% efficiency improvement over a 1:1 symmetric transmit and receive coil at the same separation.

INDEX TERMS Coil, electronic textiles, impedance matching, resonant coupling, wireless power transfer.

I. INTRODUCTION

Smart cycling has recently attracted research interest [1] with applications towards pollution monitoring, environmental sensing [2], and ground conditions monitoring for fitness applications [3]. A mechanical energy harvester on a bicycle combined with a Wireless Power Transfer (WPT) module can act as an enabling platform for wearable sensing and computing in a smart city environment [4]. Piezoelectric [5], electromagnetic [6] and switch reluctance [4] energy harvesters have been presented to harvest mechanical energy from a bicycle's motion. Wearable smart textiles, a pervasive sensing and edge-computing platform [7], [8], require power autonomy through textile-based energy harvesting, or Wireless Power Transfer (WPT) in the near or far-field [9]. In future smart cities, energy harvested from cycling can be transferred wirelessly to on-body sensors, without the need to maintain a physical connection.

Near-field, non-radiative WPT enables high efficiency transmission of energy without wires. For example, resonant and non-resonant inductive coupling are widely utilized in consumer electronics for wireless charging [10], electric vehicle and bicycle charging [11], [12], and ultra-low-power sensors and body implants [13], [14]. Furthermore, magnetic resonance (MR) WPT represents a promising solution to improve the WPT efficiency at relatively long distances with support for multiple receivers [15]–[17]. The highest efficiency wireless power transfer has been reported to take place from 1 to 10 MHz [18].

A fundamental challenge in WPT systems is designing a system that maintains high efficiency at varying coupling levels. Analytical and experimental techniques have

The associate editor coordinating the review of this manuscript and approving it for publication was Yasar Amin.

been applied to optimize the separation between the coils to achieve maximum efficiency [19]. Frequency splitting in tightly coupled WPT systems occurs due to the variation in the mutual inductance which affects the resonant frequency of the system, reducing the efficiency at the frequency of choice [20]. While frequency tracking can be used to readjust the system's frequency of operation [21], this approach requires additional control hardware to implement the feedback loop to tune an adaptive matching network [22], or a complex transmitter coil structure to accommodate the range of WPT frequencies [23]. A WPT system based on asymmetric transmit and receive coils has been demonstrated with improved resilience to frequency splitting [24].

Optimizing a WPT system for various coil separations has been investigated in [25] using variable tuning capacitor values for each operation regime. In [26], capacitive tuning of the receiver was combined with the rectifier circuit presenting a separation-independent rectifier. However, both approaches require additional circuit components such as a reflectometer, for dynamic reconfiguration of the matching network at runtime. In a wearable system, where maintaining a minimum component count is essential to the durability of the system, its integration with the fabric, and the user's comfort [27] complex control circuitry such as that realized in stationary or industrial WPT systems are not feasible. In addition, feedback loops and active tuning circuits introduce a power overhead which reduces the overall efficiency in energy harvesting systems. Therefore, a compact fully-passive tuning approach is required for energy harvesting-powered wearable WPT systems.

Flexible and textile coils for wearable WPT have been fabricated using multiple techniques: additive manufacturing using ink-jet printing or screen printing [28]–[30], embroidery [28], [31], metal-filled stretchable silicon [13], and adhered copper wires and foils [32]. Methods of minimizing the series resistance of thin embroidered coils have been presented through double sewing of the conductor [31] as well as increasing the thickness of the embroidered coil pattern [28].

The effect of different coil-fabrication techniques on the coils' inductance and resistance has been compared in [28], the efficiency of flexible coils on different substrates have been compared at a fixed distance with varying misalignment angles in [33], demonstrating 85% efficiency using a flexible PCB due to its lower dielectric losses compared to textiles, and the improved smoothness of the conductor. Multi-coil configuration have been investigated for improved resilience to misalignment [29]. The effects of human proximity on MR WPT have been extensively studied in [32], [34], [35]; up to 50% efficiency on the body at 1 cm, and 7% efficiency through a 1 cm muscle-mimicking liquid has been achieved using flat copper tape coils [35].

The interaction of WPT coils with the human body has been widely investigated [32], [34]–[38]. On the other hand, frequency splitting has not been addressed by previous wearable WPT studies. For example, the WPT efficiency of [32]–[35] were not reported in the over-coupling region. Moreover, while the effects of the body on the wireless-link efficiency has been studied [35], wearable WPT systems were not investigated in the over-coupling region, therefore neglecting the impact of coil's detuning on the WPT efficiency at very short links. Detailed interaction of WPT systems with the human body was investigated by observing the Specific Absorption Rate (SAR) for different coils while providing standard methods of evaluating compliance of WPT to regulations [37]. Along with analyzing the SAR of the proposed system, this work focuses on maximizing the on-body WPT efficiency through improved coil tuning that is resilient to both detuning due to over-coupling and due to human proximity.

In this paper, a novel wearable 6.78 MHz (the Industrial Scientific and Medical, ISM-band) WPT system, fabricated using embroidered textile coils, is presented based on dual-receiver coils, and asymmetric transmitter and receiver coils for a smart cycling glove. A simple solution to over-coupling and frequency-splitting is proposed, omitting the need for adaptive impedance matching and achieving separation-independent WPT efficiency. Compared to the dynamic separation-independent systems in [20]–[23], [25], [26], this work presents the simplest receiver coil architecture with only two planar receiving coils tuned using fixed capacitor values optimized for the application's separation range. Furthermore, this work addresses the over-coupling problem in flexible and wearable WPT systems, demonstrating over $\times 5$ higher WPT efficiency in the over-coupling region, compared to a symmetric 1:1 coil without any additional tuning. Finally, the system achieves the highest reported WPT efficiency using flexible coils both in space and in human proximity, with improved immunity to varying separation both under strong and weak coupling.

This paper is structured as follows: the system requirements and the dual-receiver architecture are outlined in section II, section III discusses the coils design and fabrication, the performance of the symmetric 1:1 coils is evaluated in section V. Section VI shows the performance of the dual-receiver three-coil system as well as a comparison of the proposed system with state-of-art wearable non-radiative WPT systems.

II. DUAL-RECEIVER, SEPARATION-INDEPENDENT WEARABLE WPT

The proposed system aims to transfer the power generated from a mechanical energy harvester on a bicycle [4], to on-body textile-based sensors through the cyclist glove, utilizing strongly coupled magnetic resonance (resonant inductive coupling) between embroidered coils on the bicycle's handle and on the user's hand [4]. The main requirement is maintaining high efficiency on tight grip (approximately no separation between the transmitter and receiver coils) as well as having a high resilience to misalignment and separation over short distances. Therefore, the main challenge is optimizing a WPT system that maintains an efficiency

approaching its maximum theoretical efficiency under loose coupling while being immune to over-coupling, without the need for an adaptive impedance matching network or varying the WPT link frequency. To explain, active frequency tracking require additional complex circuitry at either the transmitter and receiver [25], [26], which are not compatible with the simple seamlessly integrated textile-based system. In addition, active tracking circuits based on amplifiers have a considerable current consumption, this makes them more applicable in high-power applications as opposed to mW energy harvesting [25], [26].

The proposed WPT system is based on dual asymmetric receiver coils for the front and back of the user's hand, aiming to maintain the input impedance matching in all modes of operation. In an inductive WPT system, the theoretical maximum efficiency (η_{WPT}) of a system is calculated using (1) from [39], where N: number of turns, α: coil radius and s: coil separation, indicating the relation between the coil size and the supported WPT distance. Thus, smaller coils are utilized for the transmitter and the close-proximity receiver for improved η_{WPT}. The large coil aims to improve the WPT coupling link at longer distance and at misalignment, as well as enables high efficiency WPT through the body. The resonance frequency of the system (2) has been set to 6.78 MHz, both the transmitters and receivers utilize lumped capacitors calculated using (3). Only the self-inductance of the coils has been considered when selecting the initial tuning capacitors. As a result, as the mutual inductance becomes more significant, frequency splitting due to detuning of the system' resonant frequency is expected due to the change in the total inductance resulting in odd and even mode resonances.

$$\eta_{WPT} = \frac{\mu_0^2\pi^2 N_{TX}^2 N_{RX}^2 \alpha_{TX}^4 \alpha_{RX}^4 \omega^2}{16 R_{TX} R_{RX} (\alpha_{TX}^2 + s^2)^3} \tag{1}$$

$$f_r = \frac{1}{2\pi\sqrt{LC}} \tag{2}$$

$$C = \frac{1}{4\pi^2 f_r^2 L} \tag{3}$$

In resonant inductive WPT, high-Q coils are able to achieve higher WPT efficiencies over larger separations, i.e. at lower mutual inductance and hence at a lower coupling factor k. However, the system is prone to detuning, which deteriorates the efficiency, at shorter links. In order to understand the effect of shorter links on the WPT, the coupling k between the coils, (4), needs to be analyzed. The power transfer efficiency between coils is a function of the coupling mutual inductance M [20]. Critical coupling, k_c (5), describes the coupling factor at which maximum WPT efficiency is achieved [40]. When $k > k_c$, the coils operate in the over-coupling region, where the mutual inductance of the coils M affects the tuning of the coils resulting in frequency splitting, where Q can be calculated using (6), showing the dependence of k_c on both the coil's series resistance but more dominantly by the source and load impedances Z_0.

$$k = \frac{M}{\sqrt{L_{TX} L_{RX}}} \tag{4}$$

$$k_c = \frac{1}{\sqrt{Q_{TX} Q_{RX}}} \tag{5}$$

$$Q = \frac{\omega L}{R + Z_0} \tag{6}$$

M of a single turn coil, described by the Neumann equation (7), is a function of curves (C_{TX}, C_{RX}) spanning the coils of radii α, and is inversely-proportional to the separation s [19].

$$M = \frac{\mu}{4\pi} \oint_{C_{TX}} \oint_{C_{RX}} \frac{\mathrm{d}l_{TX}\,\mathrm{d}l_{RX}}{s} \tag{7}$$

From [19], equation (7) shows that it is not possible to design a 1:1 WPT system which operates at varying coil separation without implementing a feedback control loop for re-achieving resonance at the target frequency [41]. The WPT efficiency can be calculated using two-port circuit analysis based on the forward voltage transmission (S_{21}) between the coil, a function of M and Q, represented by Z_0 and R (8), the WPT efficiency can then be calculated using (9) [19].

$$S_{21}(\omega) = \frac{2jMZ_0\omega}{M^2\omega^2 + [(Z_0 + R) + j(\omega L - \frac{1}{j\omega C})]^2} \tag{8}$$

$$\eta_{WPT} = |S_{21}|^2 \tag{9}$$

To aid the theoretical analysis of the system's performance, the closed-form approximation of M in [42] was evaluated to compare the analytical results to the experimental ones in the section V. M is given by (10)-(13) as a function of the coil's geometry and separation s for coils of n turns, r_{out} radius, w track width and p track separation, where the M of the multi-turn coil is given by the sum of M_{ij} for individual loops.

$$M = \rho \times \sum_{i=n_{TX}}^{i=1} \sum_{j=n_{RX}}^{j=1} M_{ij} \tag{10}$$

$$M_{ij} = \frac{\mu_0 \pi a_i^2 b_j^2}{2(a_i^2 + b_j^2 + s^2)} \left(1 + \frac{15}{32}\gamma_{ij}^2 + \frac{315}{1024}\gamma_{ij}^4\right) \tag{11}$$

$$a_i = b_i = r_{out} - (n_i - 1)(w + p) \tag{12}$$

$$\rho = \frac{4}{\pi^2} \tag{13}$$

The main condition when using the approximation in [42] to calculate the mutual inductance is the integration over a circular loop. Therefore, the mutual inductance between rectangular coils is calculated to be $(4/\pi)^2$ times greater than circular coils. In addition, the approximation is optimized for coils with smaller radius, where M is underestimated by more than 5%, compared to 3D electromagnetic (EM) simulation, for a 5 mm radius compared to around 2% for a 3 mm coil radius. Therefore, the analytically calculated M at separation distances less than half of the coil radius is expected to be underestimated.

In this section, the 10 turns coils are assumed to have a rectangular geometry with 30 mm radius, 1-mm pitch is used for the turns separation and 40 μm-thick traces are considered. The two-port S_{21} and the approximated mutual inductance from [42] were evaluated parametrically to investigate the behaviour of the system as a function of separation and frequency, as well as a function of the systems characteristic impedance Z_0. Fig. 2-a shows the frequency-splitting phenomenon, resulting in deteriorating WPT efficiency at 6.78 MHz beyond the critical coupling point k_c, with the highest WPT efficiency shifting to the upper and lower odd and even frequency splitting modes. Therefore, it is concluded that for a distance-insensitive WPT to be realized, improved tuning is required to maintain high efficiency in the when $k > k_c$. This is presented in this work using the dual-receiver architecture, with varying receiver coil size, along with empirical tuning to overcome frequency splitting.

In this work, a WPT system of a characteristic impedance $Z_0 = 50\Omega$ is considered for compatibility with standard test instruments without the need for impedance transformers as in [19]. Nevertheless, the wireless forward transmission, given by (9), is dependent on the Z_0:M ratio. Fig. 2-b shows the variation in the WPT efficiency as a function of input impedance at variable coil separation.

In addition to the frequency-dependence described by (4)-(8), the relationship between the coil size and the separation dynamic range is non-linear; the experimental study in [43] shows the dependency of the optimal coil separation on the coil's radius, demonstrating a non-linear relation between the size of the coil and the maximum achievable WPT efficiency at various separations. Thus, the proposed system is based on a dual-receiver coils, of different radii, for operation at a wide range of air gaps and minimizing the impact of over-coupling on the dual-receiver efficiency of the system. In addition, the theoretical and experimental analysis in [44] demonstrate improved range of coil separations, as well as load resistances, with three symmetrical coils compared to a 1:1 WPT system.

Fig. 1 shows the schematic of the proposed system as well as a 3D layout of the system in operation. The performance of individual 1:1 symmetric coil WPT link of both coils are studied and compared to the dual-receiver architecture both in presence and absence of the human body. Finally, the performance improvement of the dual-receiver system through empirical tuning of the transmitter's lumped capacitor is reviewed in perspective of the three-coil on-body WPT system along with the effects of the human proximity on the quality-factor and bandwidth of the transmit and receive coils.

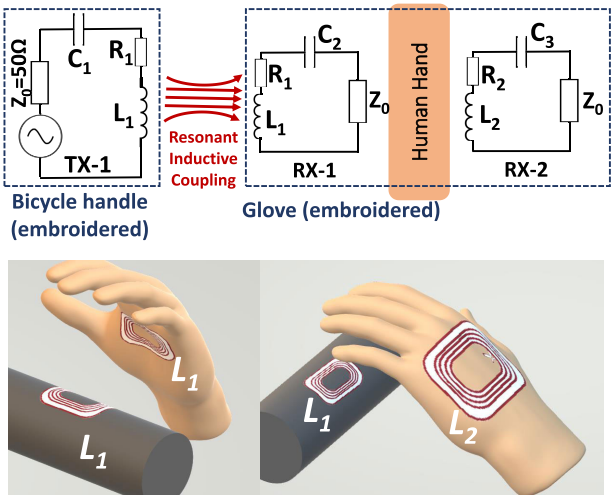

FIGURE 1. The proposed WPT system architecture: Schematic (top), showing the dual-coil receiver architecture and 3D layout (bottom) showing the coils arrangement.

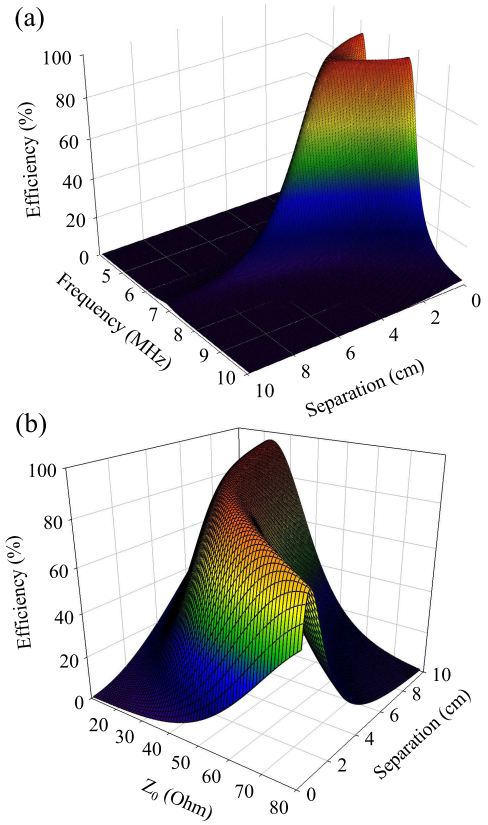

FIGURE 2. Analytically calculated WPT efficiency using the mutual inductance and the equivalent circuit S_{21}: (a) frequency splitting with over-coupling for $Z_0 = 50\Omega$, (b) effect of Z_0 on the critical coupling point at 6.78 MHz.

III. TEXTILE COIL DESIGN AND FABRICATION

A. DESIGN

As shown in Fig. 1, two coils are to be incorporated for both sides of the user's hand, with the back-hand coil having larger dimensions; benefiting from the larger available surface area to improve the WPT efficiency over longer distances or with misalignment. The inductors have been designed using EAGLE PCB CAD, with 0.04 mm track width, to match the Litz wires thickness, as discussed in the next subsection. The separation between the coil turns has been set to 1 mm to reduce fabrication inconsistencies. The inner coil radius (commonly known as the ferrite region) has been designed to be 1 cm and 2 cm for the small and large coil respectively. Fig. 3 shows the layout and dimensions of the proposed coils.

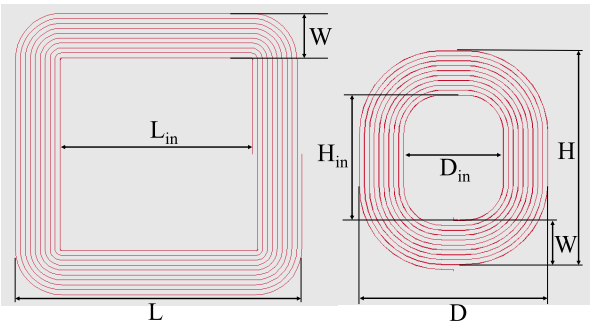

FIGURE 3. Layout of the designed 10 turns coils: L_1 (right), L_2 (left). Dimensions in mm: $L = 60, L_{in} = 40, W = 10, H = 46, H_{in} = 26, D = 40, D_{in} = 20$.

B. FABRICATION

Multiple methods have been proposed for fabricating coils for flexible wearable WPT systems as discussed in the introduction. In this work, automated embroidery is utilized to stitch the conductor traces. Commercially available 40 μm thick silk-coated copper Litz wires are selected for the conductive traces, for reduced high-frequency resistance due to skin effect. The coils have been directly embroidered to a 0.266 mm-thick polyester-cotton substrate ($\epsilon_r = 1.6$, $tan\delta = 0.027$). An automated sewing machine (PFAFF Creative 3.0) has been used to automatically embroider the conductive traces on the textile substrate. Compared to printed and ablated planar rectangular coils, a planar coil formed out of a Litz wire is expected to achieve lower resistance hence improving the WPT efficiency [28]. A maximum variation of 4% has been observed in the measured inductance of four coils fabricated using the same approach. Fig. 4 shows a photograph of the fabricated textile coils.

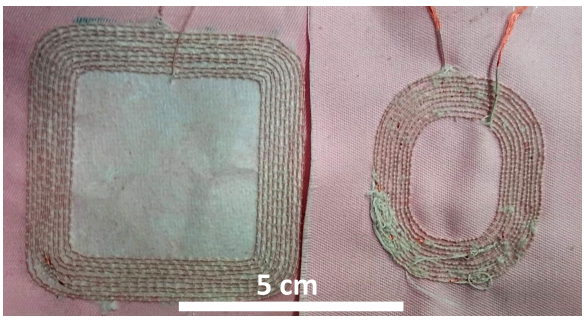

FIGURE 4. Photograph of the embroidered WPT textile coils, A: transmitter and primary receiver coil (right), B: secondary, large, receiver coil (left).

The unloaded coil parameters: series resistance R and inductance L were measured from 0.1-10 MHz using a WK 6500B impedance analyzer, the quality factor Q was calculated using $Q = \omega L/R$ at 6.78 MHz. Table 1 shows a comparison of the fabricated coils parameters with reported wearable WPT coils. It can be observed that the proposed embroidered coils have lower series resistance compared to printed planar coils due to the Litz/silk conductors utilized, allowing higher WPT efficiency based on (1).

TABLE 1. Comparison of the fabricated coils measured parameters with reported flexible WPT coils.

	L_1	L_2	[28]	[28]
Dim. (mm)	40×46	60×60	Dia.=138	Dia.=90
Q	361	339	151	347
L (μH)	3.9	10.2	3.9	9.8
R (Ω)	0.46	1.28	1.1	1.2
Fabrication	Embroidered textile	Embroidered textile	Screen printed on textile	Sewn Litz on textile

IV. WPT EXPERIMENTAL SETUP

For evaluating the WPT performance of the designed coils, 50 Ohm solder-terminated SMA connectors were incorporated for exciting the transmitter/receiver coils using a two-port vector network analyzer (VNA). The VNA (Rhode and Schwarz ZVB4) has been set to transmit at 10 dBm and was used to measure the WPT efficiency from the forward transmission s-parameter (S_{21}). The S_{21} has then been converted to the power-wave transfer function to calculate the power transfer ratio, ($\eta_{WPT} = |S_{21}|^2$). Multiple investigations were carried out to understand the impact of different variations in separation and alignment, both in presence and absence of the body for the two-coil system. The proposed dual-receiver is then implemented and evaluated both in free space and on hand. Fig. 5 shows the experimental setups investigated in this work. Experiments a-d were carried out for both coils, $L_1 : L_1$ and $L_2 : L_2$, (section V the details of the implementation of each)

V. 1:1 TEXTILE COIL WPT EFFICIENCY

A. COIL SEPARATION STUDY

To measure the 1:1 symmetric coils WPT efficiency (Fig. 5-a), the two coils-under-test have been placed on a wooden test fixture to control the separation distance while performing the two-port measurements. The separation between the coils has been varied between 0.1 cm and 10 cm in free space, and between 0.5 cm and 10 cm through a tissue-mimicking model. Fig. 6 shows the WPT efficiency of the designed coils at varying distance.

As predicted from (1), the larger coils, benefiting from larger radius achieve a higher maximum efficiency of 82.6% compared to 65.9% by the small coils. On the other hand, due to the increased mutual inductance and hence coupling factor, the larger coils suffer from reduced efficiency at 6.78 MHz in the over-coupling region due to frequency splitting. Although a similar effect is observed with the smaller coils, they maintain 27% efficiency at no separation between the coils, demonstrating their suitability for the short WPT distance between the bicycle's handle and the glove on tight grip. The over-coupling region of the small and large coils are observed to be $0 < s < 1.5$ and $0 < s < 3.5$ cm, respectively. The maximum achievable WPT efficiency has also been measured to demonstrate the ideal system's performance assuming an impedance matching circuit is implemented to allow high efficiency operation under all coupling conditions.

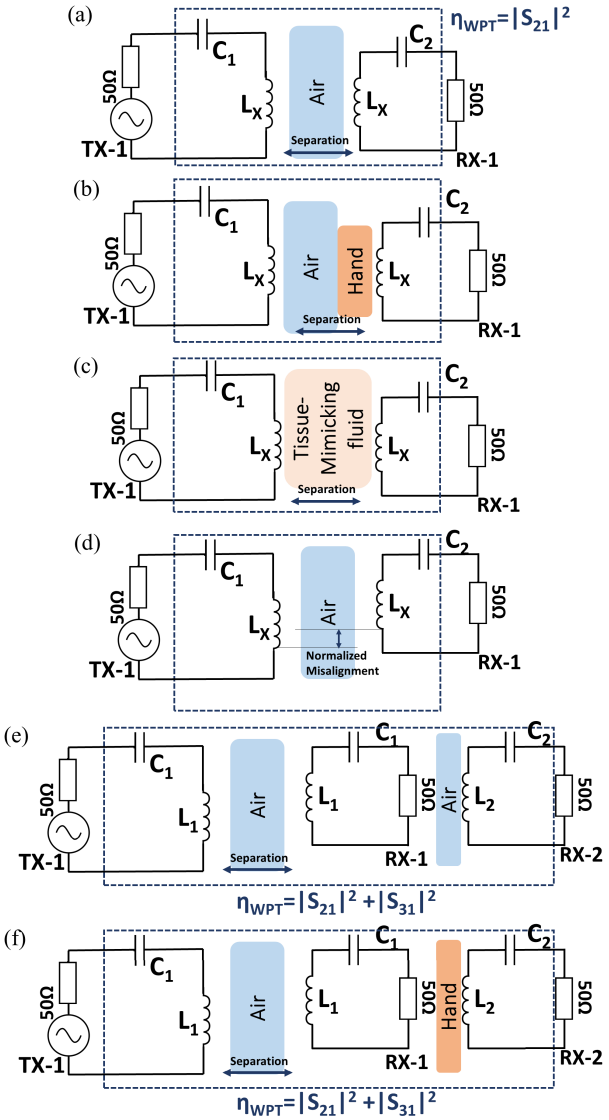

FIGURE 5. Experimental setups: (a) symmetric TX/RX in space, (b) symmetric TX/RX on the back of the hand, (c) symmetric TX/RX through body-mimicking fluid, (d) normalized misalignment of symmetric coils, (e) dual-receiver system in space, (f) dual-receiver system with on-hand RX.

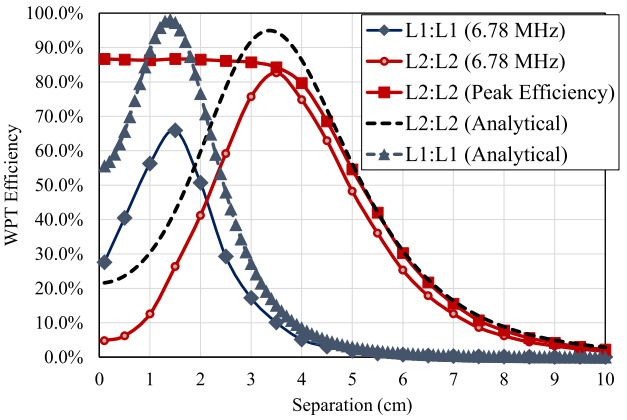

FIGURE 6. Measured and calculated WPT efficiency, aligned in space, of the proposed coils at varying coil separation distances; test setup a from Fig. 5.

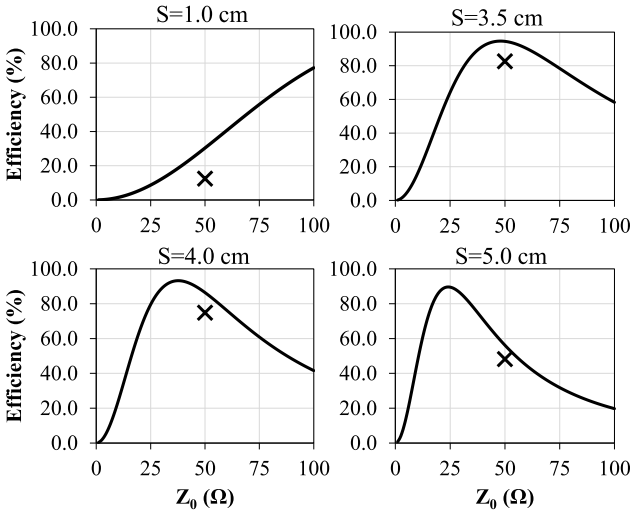

FIGURE 7. Analytically calculated (solid line) and measured (discrete 50Ω point) L2:L2 WPT efficiency as a function of the input system's characteristic impedance at various separations: (1 cm) over-coupling, (3.5 cm) critically coupled, (4 cm) under-coupled, (5 cm) under-coupled.

It is observed that for the L2:L2 case, the analytical and measured results agree in the under-coupled region. However, the higher discrepancy at $S < 3.5$ cm can be attributed to eq. (10) being specifically tuned to coils of $r < 5$mm. In addition, [42] shows that the error margin compared to EM simulation increases at separations under 1 cm for a coil of 5 mm radius.

The highest discrepancy in efficiency between the calculated and measured result is observed for the L1:L1 case (the small coils). The agreement of the calculated and measured separation at which critical coupling occurs validates the M calculation. Therefore, the only source of uncertainty in (8) is R. To explain, while the resistance of the coil has been measured, the tuning capacitor's parasitic resistance remains unknown and at a high frequency, can be in the range of 1-10 Ω. This is less evident in the large coil (L2) case where the tuning capacitor used is smaller than that of the small coil (L1) due to the coil's lower inductance. Thus, for higher WPT efficiencies to be achieved using a smaller coil, lumped capacitors of higher Q can be used.

The experimental setup, Fig. 5, is fixed to 50Ω characteristic impedance (Z_0). However, as observed in Fig. 2-b, the characteristic impedance affects the critical coupling and hence the optimal separation of the coils. Eq. (8) was used to calculate the analytical WPT efficiency as a function of the characteristic impedance, which requires complex source and load-pull instrumentation to be measured experimentally. Fig. 7 shows the calculated WPT efficiency variation with Z_0 and the measured efficiency at $Z_0 = 50\Omega$.

It is observed that using a system of lower Z_0, critical coupling can be maintained at lower coupling factors and hence higher coil separations. This is explained by (5)-(6) which show the direct dependence of k_c on Z_0. For example,

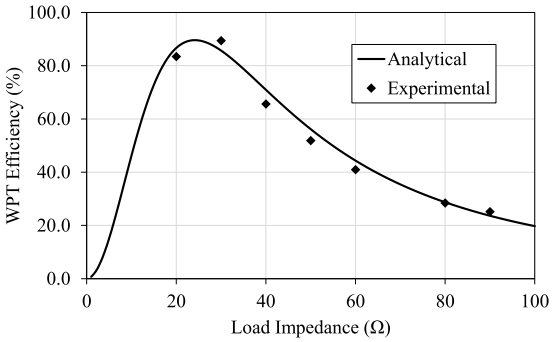

FIGURE 8. Measured and analytically calculated WPT efficiency as a function of the load impedance, at 5 cm coil separation.

the 83% critical-coupling WPT efficiency of the system can be maintained at 5 cm separation if Z_0 of the source and load is transformed to 25Ω. For practical systems, this can be achieved using a standard impedance transformer such as an L-network.

To validate the theoretical calculations of the impact of the load resistance on the WPT link, the 50Ω load termination has been replaced with a variable resistor. The voltage across the load resistor has been measured using a ×10 oscilloscope probe with a 1-MΩ termination. Fig. 8 shows the calculated and measured WPT efficiency as a function of the load impedance, in a typical under-coupled WPT scenario at 5 cm separation.

In addition to the two-port measurements of the WPT efficiency using a VNA, experimental validation using different wave-forms have been carried out to observe the system's performance in time-domain. A 50Ω signal generator has been used to transmit at 10 dBm, an oscilloscope with 50Ω termination has been used to observe the output. Continuous Wave (CW) excitation using a sine-wave and a square wave have been considered. Fig. 9 shows the measured input and output wave-forms as viewed on the oscilloscope.

While the single-ton sine-wave closely matches with the predicted values, the square wave excitation is expected to be distorted as observed on the scope. To explain, as a square wave is composed of a sum of multiple sinusoidal waves, the resonance at 6.78 MHz implies that the sine-waves near the system's resonance frequency will be transmitted to the output.

B. WPT IN PRESENCE OF HUMAN TISSUE

In the proposed system, the large coil is positioned behind the user's hand. Therefore, the WPT efficiency of the large coil needs to be quantified in presence of the hand, for a more accurate evaluation compared to the body-mimicking fluid scenario. Fig. 10 shows the WPT efficiency of the large coils with the transmitter placed on top of the user's hand (Fig. 5-b). Although the efficiency drops due to absorption by the tissues, the human hand improved the WPT efficiency of the coil in the over-coupling region (s = 2.5 cm), by reducing the frequency splitting effect, as the high-ϵ_r

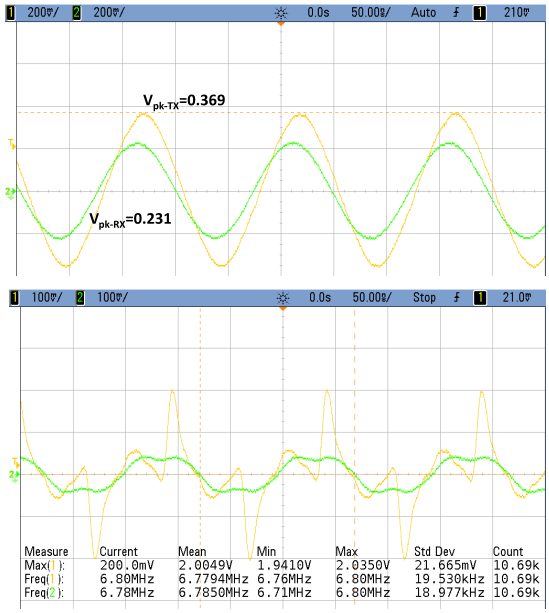

FIGURE 9. Oscilloscope traces showing the voltage across the transmitter (Channel 1) and the receiver coil (Channel 2) under CW sinusoidal excitation (top) and square wave excitation (bottom).

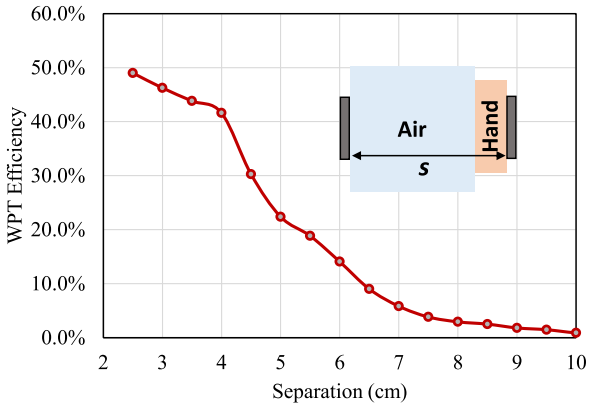

FIGURE 10. Measured WPT efficiency of the large coil placed behind the user's hand, at varying distance from the transmitter, the 2.5 cm minimum distance is capped by the thickness of the hand; test setup b from Fig. 5.

medium reduces the mutual inductance of the coils. While this is expected to reduce the efficiency, as observed with the smaller coil, the larger coil maintained its resonant frequency hence improving its efficiency by 10% in the over-coupling region.

In EM systems operating in vicinity of the human body the safety regulations requirements regarding exposure limits and field distributions need to be met. A 3D model of the coils separated by 2 cm of human tissue has been modelled and simulated in CST Microwave Studio, to imitate the through-hand WPT scenario. The model shown in Fig. 11 utilizes a simplified hand model based on CST's Voxel tissue library widely used in RF and microwave WPT [45] in addition to Body Area Networks antenna models [46].

At 6.78 MHz, the simulated WPT efficiency was 56.5%, showing a fair agreement with the measured efficiency.

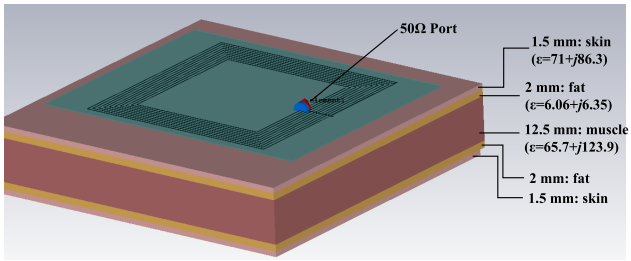

FIGURE 11. CST EM simulation model of the coils on the human-body model.

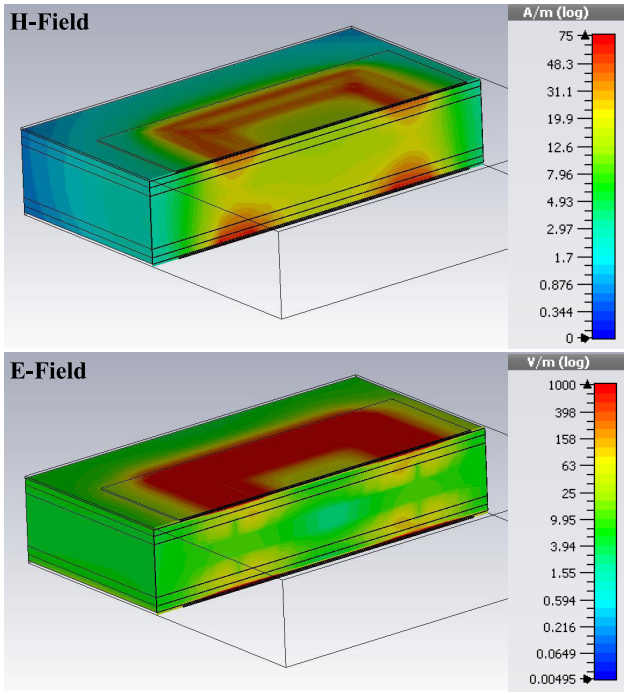

FIGURE 12. Simulated maximum H-field (top) and E-field (bottom) distributions across the coils and the human hand model.

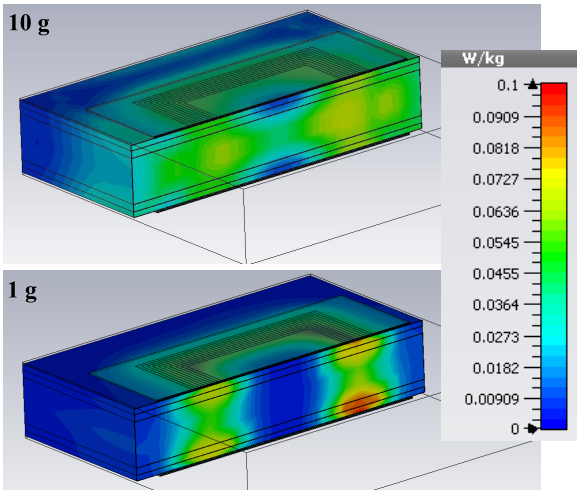

FIGURE 13. Simulated SAR using the human hand model in CST, showing a peak SAR = 0.070 and 0.103 W/kg for a 10 gm and 1 gm sample, respectively.

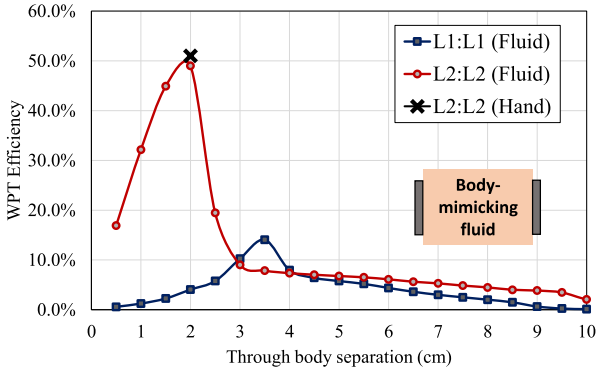

FIGURE 14. Measured WPT efficiency, through body-mimicking fluid, of the proposed coils at varying coil separation distances; test setup c from Fig. 5.

Compared to the measured 51% across a real human hand and using lumped components, the higher simulated efficiency can be attributed to modelling the lumped capacitor as an ideal component; using real-lumped capacitors, a portion of the transmitted power is expected to be absorbed in the capacitors' internal series resistance. CST field monitors were used to calculate the power dissipated in the materials at 6.78 MHz. Only 1.16% of the 0.5 W excitation signal has been absorbed by the human tissue implying minimal interaction between the hand and the coils. Fig. 12 shows the computed electric- (E) and magnetic- (H) field distribution at the center of the coils and through the human tissue.

By monitoring the power losses in human tissue at 6.78 MHz, the SAR can be calculated. Both 10-gm and 1 gm normalizations were simulated in CST to ensure compliance of the proposed WPT system with SAR regulations. The maximum computed SAR is under 0.103 W/kg for both cases, well below the regulatory limit of 1.6 W/kg [38]. Fig. 13 shows the maximum SAR plot across the human hand model.

In order to investigate the WPT efficiency of the presented coils through the human body at varying coil-separation, a compressible sac of tap water has been used to mimic human tissue of varying thickness to investigate the efficiency of the WPT link through the body (Fig. 5-c). Although commercial body phantoms can be utilized to obtain more precise results for body-plantar applications especially at higher frequencies (>100 MHz), the dielectric properties (relative permittivity and dissipation factor) of tap water ($\epsilon_r = 78$) is approximately similar to the averaged dielectric properties of different tissues such as muscle ($\epsilon_r = 112$, 27.2MHz) and fat ($\epsilon_r = 22$, 27.2MHz) [47]. Therefore, as the system is designed for operation on- and in proximity with the human body, tissue-accurate modelling of the dielectric properties of the body is not required. The measured WPT efficiency of the large coils at 2.5 cm with the human hand (no separation between the coils apart from the hand) agrees with the efficiency at 2.2 cm through the fluid (Fig. 10 and 14). At higher separation distances, the fluid model results in higher degradation in efficiency due to filling up the WPT

medium entirely, mimicking WPT through larger human organs or to an implant.

The improvement in the WPT efficiency at 2 cm through the fluid, compared to the efficiency in space, represents a close match with the results observed with the human hand (in Fig. 10) due to the isolation effect explained previously. At s = 2.5 cm to s = 6 cm, the effect of transferring the power through the body is most prevalent compared to through air, reducing the efficiency by up to 36%. It can be concluded from comparing the through-hand and through-body fluid results, that the effects of a small air gap (up to 2.5 cm air gap in this study) is minimal compared to the losses due to the tissue.

C. MISALIGNMENT STUDY

The separation between the coils has been fixed at 1.5 cm for the misalignment study. The misalignment between the coils, normalised to the coils' radii, has been varied between 0 (no misalignment) to 1 (coils displaced by distance = coil radius). Fig. 15 shows the effect of normalised misalignment on the proposed coil.

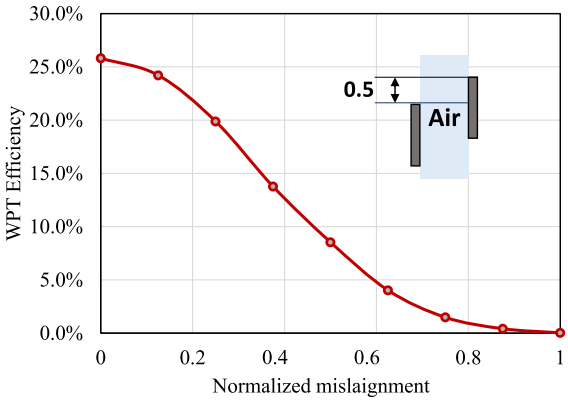

FIGURE 15. The effect of varying misalignment (normalized to the coil's dimension) on the WPT at a fixed distance; test setup d from Fig. 5.

Although the experimental results indicate that the tolerance of the coils to misalignment, when normalised to their size, is dimensions-agnostic, the size of the larger coil offers the user higher positioning flexibility. Therefore, the proposed bigger coil will reduce the impact of the user's hand misalignment with respect to the bicycle's transmitting coil.

VI. DUAL-RECEIVER INDUCTIVE POWER TRANSFER

The smaller coil operates better at a shorter WPT link due to the lower mutual inductance resulting in reduced frequency-splitting at the same distance. In this section, the dual receiver architecture is evaluated. The system is defined as a three-port network, with the transmitter acting as port-1, the small coil acting as port-2, and the large coil (at the back of the hand) acting as port-3. The power reception at both ports is measured sequentially, under the same test conditions, using the two-port VNA. The unmeasured port is

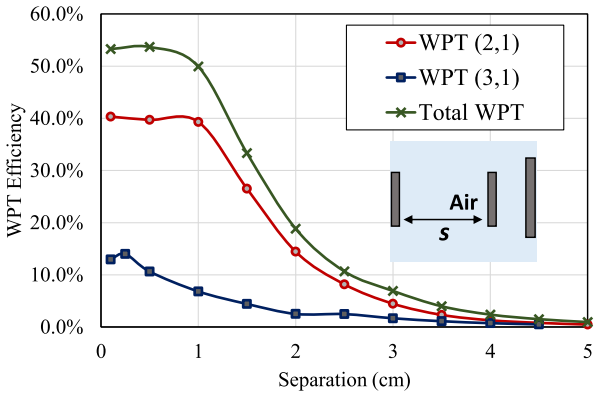

FIGURE 16. Measured WPT efficiency, in space, of the three-coil system tuned using only self-inductance of the coils (equation 3); test setup e from Fig. 5.

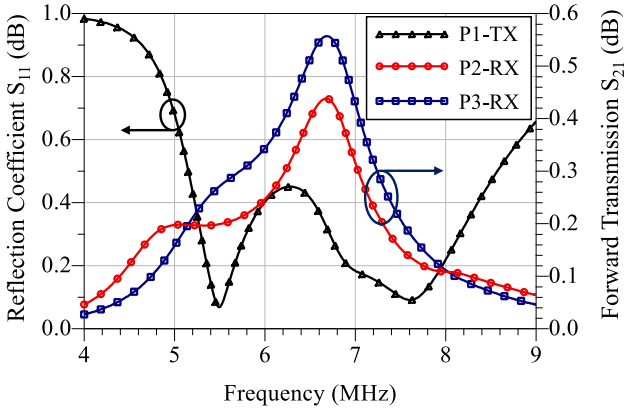

FIGURE 17. Three port s-parameters of the system with the original tuning capacitance showing frequency splitting due to the mutual inductance; test setup e from Fig. 5.

terminated using a 50-Ohm load to accurately account for the power delivered to it during normal operation.

To investigate the effects of varying separation in absence of the body, the receivers were kept at a fixed distance of 2.2 cm from each other (representing the hand thickness) while varying the separation s, measured between the small coils as depicted in Fig. 16. Ideal power combining of the two receiver coils is assumed, hence, the total WPT efficiency has been calculated as the sum of the power received by individual coils. In [48], a 6.78 MHz power combiner has been reported with and efficiency of 85.7% capable of combining power levels higher than 100W.

The dual-coil receiver architecture achieves 53% efficiency at sub-10 mm separation, the tight-coupling region, demonstrating a 48.2% and 21.6% higher WPT efficiency compared to the symmetric large and small coils respectively, as observed in Fig. 16. Nevertheless, the maximum efficiency (at 1-3 cm separation for both coils) has been capped at 54% instead of the previously achieved 82.6% by the large coil. This is attributed to the loading effect of the coils affecting the mutual inductance and hence, the impedance matching, resulting in frequency splitting due to detuning

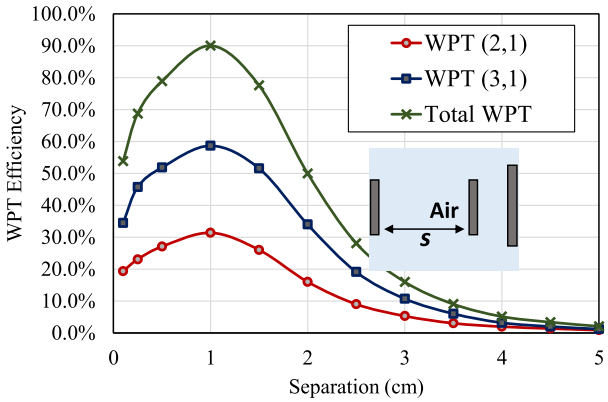

FIGURE 18. Measured WPT efficiency, in space, of the three-coil system after empirically tuning the transmitter, C_2.

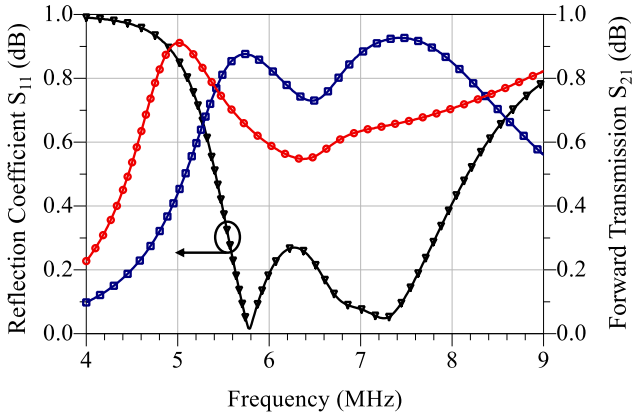

FIGURE 19. Three port s-parameters of the proposed system with the empirically selected C_1 showing improved impedance matching at 6.78 MHz. (Legend shown in Fig. 17); test setup e from Fig. 5.

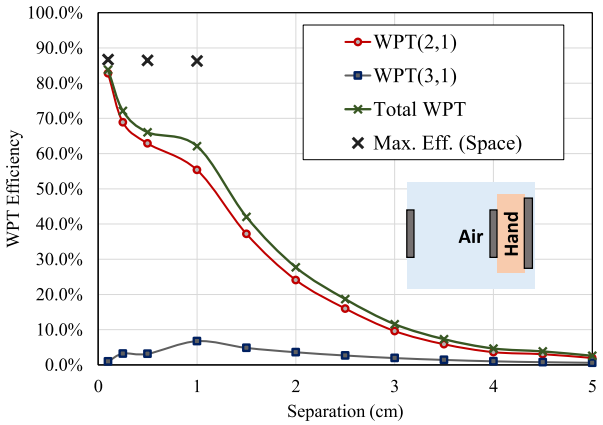

FIGURE 20. Measured WPT efficiency, on the user's hand, of the three-coil system after empirically tuning the transmitter, C_2, showing the achieved on-body WPT efficiency approaching the maximum achievable WPT in space due to the improved impedance matching; test setup f from Fig. 5.

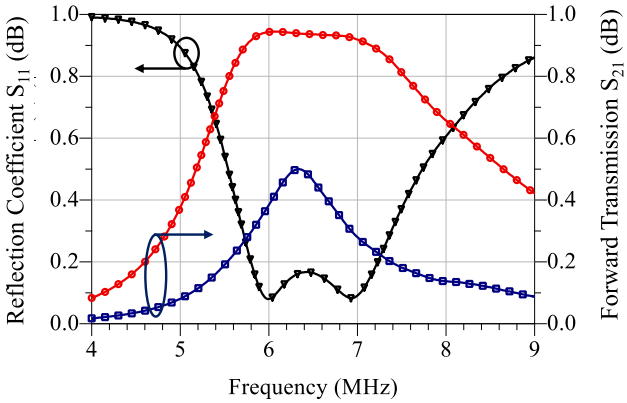

FIGURE 21. Three port s-parameters of the WPT system on the user's hand, showing 2 MHz ($|S_{11}| < 0.5$) bandwidth due to the reduced coil Q-factor. (Legend shown in Fig. 17); test setup f from Fig. 5.

of the transmitter. Fig. 17 shows the three-port s-parameters of the network at 1 cm separation, showing the maximum WPT occurring at the odd and even modes instead of the fundamental frequency. A relatively high reflection coefficient, $S_{11} = -8$ dB, is measured at 6.78 MHz explaining the deterioration in performance.

In order to re-achieve resonance at 6.78 MHz, the value of C_1, the transmitter's resonance capacitor, has been tuned empirically to shift the even-mode frequency-splitting resonance (f_{even}), which can be calculated using (14), to 6.78. As seen in Fig. 18, the empirically tuned three-coil system achieves the highest WPT efficiency in this study, 90%, due to the transmitter coil resonating at 6.78 MHz after re-tuning the capacitors in the WPT link previously affected by frequency splitting. The efficiency is no longer capped by the geometry of the smaller adjacent coil, demonstrating the benefits of the larger second receiver, which is responsible for receiving 58.7% of the power. Finally, the frequency splitting effect, previously endured by the larger coil, is mitigated by the isolation from increased mutual inductance with the transmitter due to the intermediate coil. Fig. 19 shows the s-parameters of the system after being tuned for improved impedance matching in the tight-coupling region, resulting in $S_{11} = -19.6$ dB at 6.78 MHz.

$$f_{\text{odd}} = \frac{1}{2\pi\sqrt{(L+M)C}},\ f_{even} = \frac{1}{2\pi\sqrt{LC}} \tag{14}$$

The dual-RX system has been evaluated in presence of the human hand. Fig. 20 shows the WPT efficiency of the system on the user's hand. 83.8% efficiency, the highest observed on-body WPT efficiency in this study is due to achieving the frequency splitting resonance at 6.78 MHz at the shortest transfer distance. This is attributed to the wide resonance bandwidth observed at the input, Fig. 21, due to the reduced Q-factor of the loaded coils. The short-link WPT efficiency improvement in human proximity, discussed in the previous section, re-manifests at 0.1 cm separation resulting in 30% higher efficiency. Moreover, the inverse-proportionality with separation stagnates between 0.2 cm and 1 cm as observed with the 1:1 large coil on hand. A comparison of the proposed system with reported state-of-art non-radiative wearable and

TABLE 2. Comparison of the proposed textile WPT system with wearable WPT SoA.

	This Work	2016 [35]	2017 [33]	2019 [34]	2019 [34]	2018 [28]
WPT Method	Dual-RX strongly coupled MR	MR	MR	Strongly coupled MR	Strongly coupled MR	Inductive coupling
Optimal S (cm)	0.5-2	3-7	0-8†	6	6	0.5-2
Coil design	Planar rectangular/spiral, dual-RX coils	Planar spiral, dual-TX oils	Planar loop TX, spiral resonator	Planar circular, Resonator+load loop	Planar circular, Resonator+load loop	Planar spiral
Coil size (cm)	TX: 4.6 × 4 RX: 6 × 6	Diameter_{TX}=10, Diameter_{RX}=9	Diameter=9	Diameter=3.2	Diameter=3.2	Diameter=9
Coil fabrication	Embroidered Litz wires	Copper foil on polyester	1 mm wire on textile	Conductive high ρ textile	Flex PCB	Sewn Litz wires
Freq. (MHz)	6.78	6.78	6.28 and 9.29	80	80	0.11 to 0.205
η_{space}	91% (S=1)	60% (S=3)	NR	60%	80%	55% (S=1)
$\eta_{on-body}$	64%* (S=1)	52%**	75%	44%*‡	66%*‡	NR
$\eta_{through-body}$	49%**, (S=2)	6.87%**	NR	NR	NR	NR

*Measured on hand. **Measured through body-mimicking fluid. † Does not include frequency shifting effects. ‡ Measured using a 12-layer FR4 TX.

flexible WPT systems is presented in table 2, demonstrating the highest reported WPT efficiency both on- and off-body.

VII. CONCLUSION

In this paper, a compact dual-receiver WPT system is presented for maximizing the WPT efficiency under varying operation conditions, achieving separation-independent operation in the over-coupling region. Detailed analytical and experimental analysis of the frequency-splitting and over-coupling phenomena are presented to overcome the separation-dependent losses in WPT applications. A novel application, wearable smart cycling gloves, is presented to demonstrate efficient power transfer regardless of variation in coil-separation, misalignment and human-proximity through a simple impedance matching technique. The proposed dual-receiver system achieves a peak efficiency of 90% and 82% in space and on-hand, respectively, a 40% WPT efficiency improvement compared to standard 1:1 symmetric coils. This is the highest reported WPT efficiency for an on-body flexible wearable WPT system and the first investigation of the over-coupling problem in wearable WPT.

Although the presented system and design approach have been demonstrated for wearable applications, with focus on the effects of the human body being the WPT medium, the proposed tuning method can be applied to dynamic WPT applications where maintaining a certain level of separation-independence is a requirement. The impact of the transmitter coil's Q-factor on the impedance matching, as well as the coil's bandwidth in human-proximity could be utilized in designing separation-independent WPT systems for industrial applications such as non-stationary WPT links, where the WPT medium is changing; eliminating the need for additional feedback loops, adaptive matching networks, and frequency-tuning circuitry.

ACKNOWLEDGMENT

Datasets supporting this article are available from the University of Southampton Repository at DOI: 10.5258/SOTON/1217.

REFERENCES

[1] O. B. Piramuthu, "Connected bicycles—State-of-the-art and adoption decision," *IEEE Internet Things J.*, vol. 4, no. 4, pp. 987–995, Apr. 2017.

[2] X. Liu, C. Xiang, B. Li, and A. Jiang, "Collaborative bicycle sensing for air pollution on roadway," in *Proc. IEEE 12th Int. Conf. Ubiquitous Intell. Comput., IEEE 12th Int. Conf. Autonomic Trusted Comput., IEEE 15th Int. Conf. Scalable Comput. Commun. Associated Workshops (UIC-ATC-ScalCom)*, Aug. 2015, pp. 316–319.

[3] Y.-X. Zhao, Y.-S. Su, and Y.-C. Chang, "A real-time bicycle record system of ground conditions based on Internet of Things," *IEEE Access*, vol. 5, pp. 17525–17533, 2017.

[4] W. Komolafe, M. Wagih, A. Valavan, Z. Ahmed, A. Stuikys, and B. Zaghari, "A smart cycling platform for textile-based sensing and wireless power transfer in smart cities," *Proceedings*, vol. 32, no. 1, p. 7, Dec. 2019.

[5] E. Minazara, V. Dejan, and F. Costa, "Piezoelectric generator harvesting bike vibrations energy to supply portable devices," in *Proc. Int. Conf. Renew. Energies Power Qual. (ICREPQ)*, 2008, pp. 1–6.

[6] L. Buccolini and M. Conti, "An energy harvester interface for self-powered wireless speed sensor," *IEEE Sensors J.*, vol. 17, no. 4, pp. 1097–1104, Feb. 2017.

[7] L. Zhang, Z. Wang, and J. L. Volakis, "Textile antennas and sensors for body-worn applications," *IEEE Antennas Wireless Propag. Lett.*, vol. 11, pp. 1690–1693, 2012.

[8] J. Cheng, P. Lukowicz, N. Henze, A. Schmidt, O. Amft, G. A. Salvatore, and G. Troster, "Smart textiles: From niche to mainstream," *IEEE Pervas. Comput.*, vol. 12, no. 3, pp. 81–84, Jul. 2013.

[9] K. W. Lui, O. H. Murphy, and C. Toumazou, "A wearable wideband circularly polarized textile antenna for effective power transmission on a wirelessly-powered sensor platform," *IEEE Trans. Antennas Propag.*, vol. 61, no. 7, pp. 3873–3876, Jul. 2013.

[10] S. Y. Hui, "Planar wireless charging technology for portable electronic products and Qi," *Proc. IEEE*, vol. 101, no. 6, pp. 1290–1301, Jun. 2013.

[11] S. Li and C. C. Mi, "Wireless power transfer for electric vehicle applications," *IEEE J. Emerg. Sel. Topics Power Electron.*, vol. 3, no. 1, pp. 4–17, Mar. 2015.

[12] H. Z. Z. Beh, G. A. Covic, and J. T. Boys, "Wireless fleet charging system for electric bicycles," *IEEE J. Emerg. Sel. Topics Power Electron.*, vol. 3, no. 1, pp. 75–86, Mar. 2015.

[13] M. Manoufali, K. Bialkowski, B. Mohammed, and A. Abbosh, "Wireless power link based on inductive coupling for brain implantable medical devices," *IEEE Antennas Wireless Propag. Lett.*, vol. 17, no. 1, pp. 160–163, Jan. 2018.

[14] H. Rahmani and A. Babakhani, "A dual-mode RF power harvesting system with an on-chip coil in 180-nm SOI CMOS for millimeter-sized biomedical implants," *IEEE Trans. Microw. Theory Techn.*, vol. 67, no. 1, pp. 414–428, Jan. 2019.

[15] A. P. Sample, D. A. Meyer, and J. R. Smith, "Analysis, experimental results, and range adaptation of magnetically coupled resonators for wireless power transfer," *IEEE Trans. Ind. Electron.*, vol. 58, no. 2, pp. 544–554, Feb. 2011.
[16] B. L. Cannon, J. F. Hoburg, D. D. Stancil, and S. C. Goldstein, "Magnetic resonant coupling as a potential means for wireless power transfer to multiple small receivers," *IEEE Trans. Power Electron.*, vol. 24, no. 7, pp. 1819–1825, Jul. 2009.
[17] M. Fu, H. Yin, and C. Ma, "Megahertz multiple-receiver wireless power transfer systems with power flow management and maximum efficiency point tracking," *IEEE Trans. Microw. Theory Techn.*, vol. 65, no. 11, pp. 4285–4293, Nov. 2017.
[18] J. Yu, D. G. Hasko, and A. Nathan, "Frequency selection for high efficiency wireless power transfer," *J. Display Technol.*, vol. 12, no. 7, pp. 681–684, Jul. 2016.
[19] T. Imura and Y. Hori, "Maximizing air gap and efficiency of magnetic resonant coupling for wireless power transfer using equivalent circuit and Neumann formula," *IEEE Trans. Ind. Electron.*, vol. 58, no. 10, pp. 4746–4752, Oct. 2011.
[20] Y. Zhang and Z. Zhao, "Frequency splitting analysis of two-coil resonant wireless power transfer," *IEEE Antennas Wireless Propag. Lett.*, vol. 13, pp. 400–402, 2014.
[21] W. Fu, B. Zhang, and D. Qiu, "Study on frequency-tracking wireless power transfer system by resonant coupling," in *Proc. IEEE 6th Int. Power Electron. Motion Control Conf.*, May 2009, pp. 2658–2663.
[22] J. Park, Y. Tak, Y. Kim, Y. Kim, and S. Nam, "Investigation of adaptive matching methods for near-field wireless power transfer," *IEEE Trans. Antennas Propag.*, vol. 59, no. 5, pp. 1769–1773, May 2011.
[23] W.-S. Lee, W.-I. Son, K.-S. Oh, and J.-W. Yu, "Contactless energy transfer systems using antiparallel resonant loops," *IEEE Trans. Ind. Electron.*, vol. 60, no. 1, pp. 350–359, Jan. 2013.
[24] Y.-L. Lyu, F.-Y. Meng, and Q. Wu, "Frequency splitting elimination in wireless power transfer using nonidentical resonant coils," in *Proc. Asia–Pacific Microw. Conf. (APMC)*, Dec. 2015, pp. 1–3.
[25] D.-G. Seo, S.-H. Ahn, J.-H. Kim, W.-S. Lee, S.-T. Khang, S.-C. Chae, and J.-W. Yu, "Power transfer efficiency for distance-adaptive wireless power transfer system," in *Proc. Int. Appl. Comput. Electromagn. Soc. Symp. (ACES)*, Mar. 2018, pp. 1–2.
[26] A. P. Sample, B. H. Waters, S. T. Wisdom, and J. R. Smith, "Enabling seamless wireless power delivery in dynamic environments," *Proc. IEEE*, vol. 101, no. 6, pp. 1343–1358, Jun. 2013.
[27] A. Komolafe, R. Torah, Y. Wei, H. Nunes-Matos, M. Li, D. Hardy, T. Dias, M. Tudor, and S. Beeby, "Integrating flexible filament circuits for e-textile applications," *Adv. Mater. Technol.*, vol. 4, no. 7, Jul. 2019, Art. no. 1900176.
[28] N. J. Grabham, Y. Li, L. R. Clare, B. H. Stark, and S. P. Beeby, "Fabrication techniques for manufacturing flexible coils on textiles for inductive power transfer," *IEEE Sensors J.*, vol. 18, no. 6, pp. 2599–2606, Mar. 2018.
[29] D. Zhu, N. J. Grabham, L. Clare, B. H. Stark, and S. P. Beeby, "Inductive power transfer in e-textile applications: Reducing the effects of coil misalignment," in *Proc. IEEE Wireless Power Transf. Conf. (WPTC)*, May 2015, pp. 1–4.
[30] I. Ortego-Isasa, K. P. Benli, F. Casado, J. I. Sancho, and D. Valderas, "Topology analysis of wireless power transfer systems manufactured via inkjet printing technology," *IEEE Trans. Ind. Electron.*, vol. 64, no. 10, pp. 7749–7757, Oct. 2017.
[31] D. Sun, M. Chen, S. Podilchak, A. Georgiadis, Q. S. Abdullahi, R. Joshi, S. Yasin, J. Rooney, and J. Rooney, "Investigating flexible textile-based coils for wireless charging wearable electronics," *J. Ind. Textiles*, Feb. 2019, Art. no. 152808371983108.
[32] S. H. Kang and C. W. Jung, "Textile resonators with thin copper wire for wearable MR-WPT system," *IEEE Microw. Wireless Compon. Lett.*, vol. 27, no. 1, pp. 91–93, Jan. 2017.
[33] K. Bao, C. L. Zekios, and S. V. Georgakopoulos, "A wearable WPT system on flexible substrates," *IEEE Antennas Wireless Propag. Lett.*, vol. 18, no. 5, pp. 931–935, May 2019.
[34] S. H. Kang, V. T. Nguyen, and C. W. Jung, "Analysis of MR-WPT using planar textile resonators for wearable applications," *IET Microw., Antennas Propag.*, vol. 10, no. 14, pp. 1541–1546, Nov. 2016.
[35] S. H. Kang, J. H. Choi, F. J. Harackiewicz, and C. W. Jung, "Magnetic resonant three-coil WPT system between off/in-body for remote energy harvest," *IEEE Microw. Wireless Compon. Lett.*, vol. 26, no. 9, pp. 741–743, Sep. 2016.
[36] J. Lee, K.-S. Song, and J. Choi, "Design of a side-shielded wireless power transfer coil to achieve insensitivity against the human body effect," *Microw. Opt. Technol. Lett.*, vol. 58, no. 5, pp. 1169–1173, May 2016.
[37] A. Christ, M. G. Douglas, J. M. Roman, E. B. Cooper, A. P. Sample, B. H. Waters, J. R. Smith, and N. Kuster, "Evaluation of wireless resonant power transfer systems with human electromagnetic exposure limits," *IEEE Trans. Electromagn. Compat.*, vol. 55, no. 2, pp. 265–274, Oct. 2013.
[38] H. Dinis, I. Colmiais, and P. M. Mendes, "Extending the limits of wireless power transfer to miniaturized implantable electronic devices," *Micromachines*, vol. 8, no. 12, p. 359, Dec. 2017.
[39] D. Yates, A. Holmes, and A. Burdett, "Optimal transmission frequency for ultralow-power short-range radio links," *IEEE Trans. Circuits Syst. I, Reg. Papers*, vol. 51, no. 7, pp. 1405–1413, Jul. 2004.
[40] D.-W. Seo, J.-H. Lee, and H.-S. Lee, "Optimal coupling to achieve maximum output power in a WPT system," *IEEE Trans. Power Electron.*, vol. 31, no. 6, pp. 3994–3998, Jun. 2016.
[41] W.-S. Lee, K.-S. Oh, and J.-W. Yu, "Distance-insensitive wireless power transfer and near-field communication using a current-controlled loop with a loaded capacitance," *IEEE Trans. Antennas Propag.*, vol. 62, no. 2, pp. 936–940, Feb. 2014.
[42] S. Raju, R. Wu, M. Chan, and C. P. Yue, "Modeling of mutual coupling between planar inductors in wireless power applications," *IEEE Trans. Power Electron.*, vol. 29, no. 1, pp. 481–490, Jan. 2014.
[43] Y. Li, S. Jiang, X.-L. Liu, Q. Li, W.-H. Dong, J.-M. Liu, and X. Ni, "Influences of coil radius on effective transfer distance in WPT system," *IEEE Access*, vol. 7, pp. 125960–125968, 2019.
[44] D.-W. Seo, "Comparative analysis of two- and three-coil WPT systems based on transmission efficiency," *IEEE Access*, vol. 7, pp. 151962–151970, 2019.
[45] G. Monti, D. Masotti, G. Paolini, L. Corchia, A. Costanzo, M. Dionigi, F. Mastri, M. Mongiardo, R. Sorrentino, and L. Tarricone, "EMC and EMI issues of WPT systems for wearable and implantable devices," *IEEE Electromagn. Compat. Mag.*, vol. 7, no. 1, pp. 67–77, Apr. 2018.
[46] M. Wagih, Y. Wei, and S. Beeby, "Flexible 2.4 GHz node for body area networks with a compact high-gain planar antenna," *IEEE Antennas Wireless Propag. Lett.*, vol. 18, no. 1, pp. 49–53, Jan. 2019.
[47] R. Pethig, "Dielectric properties of body tissues," *Clin. Phys. Physiol. Meas.*, vol. 8, no. 4A, pp. 5–12, Nov. 1987.
[48] U.-G. Choi and J.-R. Yang, "A 120 W class-E power module with an adaptive power combiner for a 6.78 MHz wireless power transfer system," *Energies*, vol. 11, no. 8, p. 2083, Aug. 2018.

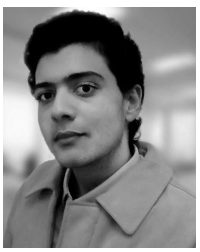

MAHMOUD WAGIH (Graduate Student Member, IEEE) received the B.Eng. degree (Hons.) from the University of Southampton, in 2018, where he is currently pursuing the Ph.D. degree.

In 2017, he worked as a Research Assistant with the University of Southampton, supported by Intel, investigating novel transmission lines. In 2018, he was a Hardware Engineering Intern with Arm, U.K. His current research interests include RF energy harvesting, wireless power transfer, mmWave wearable antennas, micro-power management, and wireless sensor networks. He has more than 15 journal and conference publications on these topics.

Mr. Wagih was a recipient of the Best Undergraduate Project Prize at the University of Southampton, in 2018, and was selected for the IEEE MTT-S IMS Project Connect, in 2019. He was also a recipient of the Best Student Paper Award (First Prize) at the IEEE MTT-S Wireless Power Transfer Conference, in 2019, and the Best Oral Paper Prize at Power MEMS, in 2019. He is a Reviewer of two IEEE journals.

ABIODUN KOMOLAFE received the B.Sc. degree (Hons.) in physics from the University of Ibadan, Nigeria, in 2007, and the M.Sc. degree in microelectromechanical systems and the Ph.D. degree in printed circuits on fabrics from the University of Southampton, in 2011 and 2016, respectively.

He is currently working as a Research Fellow with the University of Southampton, in investigating novel manufacturing methods for making functional electronics on textiles using flexible electronic circuits and screen printed electronics for medical applications. He is experienced in the design and fabrication of e-textiles using screen printing and thin film technologies.

BAHAREH ZAGHARI received the M.Sc. degree (Hons.) in electromechanical engineering from the University of Southampton, U.K., in 2012, and the Ph.D. degree in dynamic analysis of a nonlinear parametrically excited system using electromagnets from the Institute of Sound and Vibration (ISVR), University of Southampton, in 2017.

She is currently a Research Fellow with the School of Electronics and Computer Science, where she is also working on the design of smart systems, such as the next generation of jet engines and smart cities. She has industrial, consultancy, and research experience in energy harvesting and instrumentation. She has authored more than 20 articles in the area.

Dr. Zaghari has received several awards for her outstanding performance in supporting women in academia.